

## Structural and Reactivity Models for Copper Oxygenases: Cooperative Effects and Novel Reactivities

Published as part of the Accounts of Chemical Research special issue "Synthesis in Biological Inorganic Chemistry".

Joan Serrano-Plana,<sup>†</sup> Isaac Garcia-Bosch,<sup>†,‡</sup> Anna Company,<sup>\*,†</sup> and Miquel Costas<sup>\*,†</sup>

<sup>†</sup>Grup de Química Bioinorgànica, Supramolecular i Catalisi (QBIS-CAT), Institut de Química Computacional i Catalisi (IQCC), Departament de Química, Universitat de Girona, Campus Montilivi, E17071 Girona, Catalonia, Spain

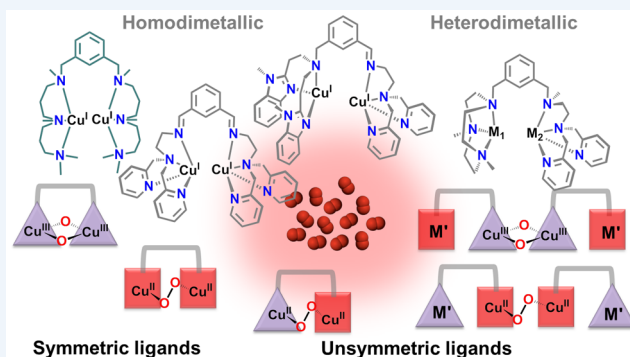
<sup>‡</sup>Department of Chemistry, Southern Methodist University, Dallas, Texas 75275-0314, United States

**CONSPECTUS:** Dioxygen is widely used in nature as oxidant. Nature itself has served as inspiration to use O<sub>2</sub> in chemical synthesis. However, the use of dioxygen as an oxidant is not straightforward. Its triplet ground-state electronic structure makes it unreactive toward most organic substrates. In natural systems, metalloenzymes activate O<sub>2</sub> by reducing it to more reactive peroxide (O<sub>2</sub><sup>2-</sup>) or superoxide (O<sub>2</sub><sup>-</sup>) forms. Over the years, the development of model systems containing transition metals has become a convenient tool for unravelling O<sub>2</sub>-activation mechanistic aspects and reproducing the oxidative activity of enzymes. Several copper-based systems have been developed within this area.

Tyrosinase is a copper-based O<sub>2</sub>-activating enzyme, whose structure and reactivity have been widely studied, and that serves as a paradigm for O<sub>2</sub> activation at a dimetal site. It contains a dicopper center in its active site, and it catalyzes the regioselective *ortho*-hydroxylation of phenols to catechols and further oxidation to quinones. This represents an important step in melanin biosynthesis and it is mediated by a dicopper(II) side-on peroxo intermediate species.

In the present accounts, our research in the field of copper models for oxygen activation is collected. We have developed *m*-xylyl linked dicopper systems that mimic structural and reactivity aspects of tyrosinase. Synergistic cooperation of the two copper(I) centers results in O<sub>2</sub> binding and formation of bis( $\mu$ -oxo)dicopper(III) cores. These in turn bind and *ortho*-hydroxylate phenolates via an electrophilic attack of the oxo ligand over the arene. Interestingly the bis( $\mu$ -oxo)dicopper(III) cores can also engage in *ortho*-hydroxylation-defluorination of deprotonated 2-fluorophenols, substrates that are well-known enzyme inhibitors. Analysis of Cu<sub>2</sub>O<sub>2</sub> species with different binding modes show that only the bis( $\mu$ -oxo)dicopper(III) cores can mediate the reaction.

Finally, the use of unsymmetric systems for oxygen activation is a field that still remains rather unexplored. We envision that the unsymmetry might infer interesting new reactivities. We contributed to this topic with the development of an unsymmetric ligand (*m*-XYL<sup>N<sub>3</sub>N<sub>4</sub></sup>), whose dicuprous complex reacts with O<sub>2</sub> and forms a *trans*-peroxo dicopper(II) species that showed a markedly different reactivity compared to a symmetric *trans*-peroxo dicopper(II) analog. Nucleophilic reactivity is observed for the unsymmetric *trans*-peroxo dicopper(II) species against electrophiles such as H<sup>+</sup>, CO<sub>2</sub> and aldehydes, and neither oxygen atom transfer nor hydrogen abstraction is observed when reacting with oxygen atom acceptors (triphenyl phosphine, sulfides) and substrates with weak C–H bonds. Instead, electrophilic monooxygenase-like *ortho*-hydroxylation reactivity is described for these unsymmetric species upon reaction with phenolates. Finally, by using a second dinucleating unsymmetric ligand (L<sup>N<sub>3</sub>N<sub>4</sub></sup>), we have described copper(I) containing heterodimetallic systems and explored their O<sub>2</sub> binding properties. Site specific metalation led to the generation of dimeric heterometallic M'<sup>II</sup>CuO<sub>2</sub>CuM' species from intermolecular O<sub>2</sub> binding at copper sites.



### 1. INTRODUCTION

Molecular O<sub>2</sub> constitutes an environmentally friendly alternative to traditional oxidants, which are still used nowadays in several chemical transformations producing large amount of waste.<sup>1</sup> The use of O<sub>2</sub> in selective oxidation processes is, however, not straightforward due to its inherent slow reactivity with most organic molecules<sup>2</sup> and the complexity of its chemistry. O<sub>2</sub> full reduction to form two water molecules is thermodynamically a very favorable 4e<sup>-</sup>/4H<sup>+</sup> process, but O<sub>2</sub> can also act as a 1 or 2e<sup>-</sup>

oxidant. Last but not least, selectivity constitutes often a critical problem in oxidations carried out by O<sub>2</sub>. Therefore, the use of O<sub>2</sub> as oxidant in organic synthesis would very much benefit from fundamental knowledge on the mechanisms of activation of this molecule.

Aerobic organisms have evolved to take advantage of the oxidizing power of O<sub>2</sub> by means of transition metals (M) that

Received: April 7, 2015

Published: July 24, 2015

reductively activate it to form  $M_n-(O_2^{\bullet-})$ ,  $M_n-(O_2^{2-})$ , or  $M_n-(O^{2-})_2$  moieties.<sup>3</sup> These redox processes are carried out in a controlled fashion in the active center of metalloproteins. In this context, copper-containing proteins are one of the most relevant subgroups of  $O_2$ -activating enzymes and a myriad of active site structures have been identified, ranging from mononuclear centers to multinuclear or heterometallic configurations.<sup>3,4</sup> This variety of structural motifs enables the performance of a wide range of reactions including oxidation, oxygenation and  $O_2$  transport. The combination of such structural and chemical diversity has fueled the interest of numerous research groups that approach this topic with different objectives, ranging from inventing new reagents for organic synthesis, exerting control over reactivity and selectivity,<sup>5,6</sup> and getting fundamental information about enzymatic reactions or basic inorganic reaction mechanisms.<sup>4,7–12</sup>

Our initial research interest in this field has targeted the study of binding and activation of dioxygen at preorganized dicopper sites, reasoning that this preorganization will be important to reproduce the structure and reactivity of type 3 copper enzymes.  $O_2$  activation at mononuclear and symmetric dinuclear copper systems has been a fast moving field,<sup>9–13</sup> and our research interests have advanced toward exploring the chemistry at unsymmetric dicopper and heterobimetallic systems, which still remains largely unexplored, under the hypothesis that these species should exhibit novel reactivity.<sup>12,14</sup> The current Account summarizes our contributions in this field.

## 2. FORMATION AND CHARACTERIZATION OF $Cu_2O_2$ ADDUCTS

Synthetic  $Cu_2O_2$  adducts are commonly prepared by reaction of a copper(I) complex with  $O_2$ . Usually, in order to reproduce the histidine-rich environment present in most copper-based  $O_2$ -activation enzymes, the copper center is surrounded by nitrogen atom donors. In this sense, the use of ligands containing secondary or tertiary amines, pyridine groups and benzimidazole units has been particularly successful in the stabilization of  $Cu_2O_2$  species. Moreover, low coordination numbers are necessary to guarantee the presence of available binding sites for interaction with external  $O_2$ . Following these general principles, a wide range of  $Cu_2O_2$  adducts have been described to date.<sup>9,10</sup>

The main strategy for the preparation of  $O_2$ -activating dicopper complexes consists in the use of mononuclear  $Cu^I$  complexes ( $LCu^I$ ) (strategy A, Scheme 1). Upon reaction with

that some control over the spatial distribution of the two metals is established. The use of *meta*-xylyl linkers has proven to be particularly effective as it locates the two copper(I) centers at a proper distance and relative orientation to interact.<sup>15–18</sup> Again, the design of dinucleating ligands with unequivalent binding sites may lead to unsymmetric  $Cu_2O_2$  units. Both strategies can be used for the preparation of heterobimetallic systems in which copper activates  $O_2$  in cooperation with a different redox active metal ion ( $M'$ ). Preparation of unsymmetric systems in general and heterobimetallic complexes in particular is inherently more complicated than synthesizing their symmetric analogues. In the case of strategy A, the challenge resides in finding complexes that preclude the formation of homometallic species, while for strategy B the most challenging aspect is to accomplish site-selective metal binding and avoid the formation of mixtures.

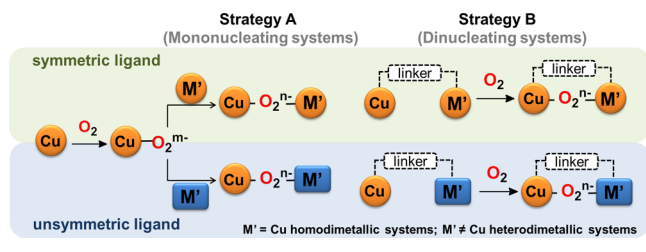
Following strategy B, we have studied the reactivity toward  $O_2$  of a series of symmetric and unsymmetric dicopper(I) and heterobimetallic complexes (Figure 1). Results are described in the following sections.

### 2.1. Illustration of Synergistic Effects in $O_2$ Binding

The reactivity of  $[Cu_2^I(Me_3m)]^{2+}$  (**1**) and  $[Cu_2^I(m\text{-XYL}^{MeAN})]^{2+}$  (**2**) with  $O_2$  (Figure 1) was compared to that of the previously reported mononuclear analogue  $[Cu^I(MeAN)]^+$  (Scheme 2).<sup>19,20</sup> The three systems presented important similarities as far as the coordination around the copper(I) center is concerned: the metal site was coordinated to three aliphatic tertiary nitrogen atoms and possessed a distorted trigonal planar geometry. Besides, copper sites in **1** and **2** could be regarded as electronically equivalent as ascertained by FT-IR analysis of their  $Cu-CO$  adducts ( $\nu(CO) = 2083$  and  $2085\text{ cm}^{-1}$ , respectively). In spite of the almost identical metal coordination structure, reactivity toward  $O_2$  was dependent on the specific ligand. Complex **1** reacted slowly with  $O_2$  even at room temperature, and no metal–oxygen adduct was detected over the course of the reaction. In contrast, reaction of **2** in acetone at  $-80\text{ }^\circ\text{C}$  was much faster and the corresponding bis( $\mu$ -oxo)dicopper(III) species (**O**), namely  $[Cu^{III}_2(\mu-O)_2(m\text{-XYL}^{MeAN})]^{2+}$  (**2<sup>O</sup>**), was obtained (Scheme 2, Figure 2a). Finally, the mononuclear analogue  $[Cu^I(MeAN)]^+$  exhibited the exclusive formation of a side-on  $\mu\text{-}\eta^2\text{-}\eta^2$ -peroxo-dicopper(II) species (**S<sub>P</sub>**) upon reaction with  $O_2$ .<sup>20,21</sup>

The different outcome of the reaction with  $O_2$  could be rationalized by taking into account a synergistic role of two copper centers in reducing the  $O_2$  molecule. The reaction in complex **1** is slower than in **2** presumably because there is an energy barrier to surmount to bring the two copper ions together, due to some strain from the ligand. In complex **2**, the ligand is flexible, allowing the two copper sites to approach close enough to promote their cooperation to bind/reduce  $O_2$ . The stability of **2<sup>O</sup>** in comparison with the lack of stability of any reaction intermediate formed along the  $1/O_2$  pathway may also be explained on the basis of the different structural constraints imposed by the macrocyclic ligands. An analogous study could be done by comparing the chemistry of dicopper(I) complexes  $[Cu_2^I(X^L)]^{2+}$  (**X3** where  $X = H, tBu, NO_2$ , Figure 1)<sup>22</sup> with that of related macrocyclic compounds based in Schiff base ligands.<sup>23</sup> Schiff base macrocyclic compounds had been extensively studied as models for dicopper  $O_2$ -binding and activating enzymes, but  $Cu_2O_2$  species could not have been identified from their reactions. Instead, compounds **X3** reacted with  $O_2$  at low temperatures to give **O** species (**X3<sup>O</sup>**). Kinetic analyses of the oxygenation reaction by stopped-flow UV–vis spectroscopy

**Scheme 1. Different Strategies to Prepare Cu-Dioxygen Adducts**



$O_2$ , a mononuclear  $Cu^{II}$ -superoxide adduct is formed, which is prone to react with a second  $L'Cu^I$  complex to form a  $Cu_2O_2$  adduct. If the two metal complexes involved are identical, a symmetric architecture is obtained but when  $L \neq L'$  an unsymmetric  $Cu_2O_2$  adduct may form. An alternative approach is the synthesis of dinucleating ligands (strategy B, Scheme 1) so

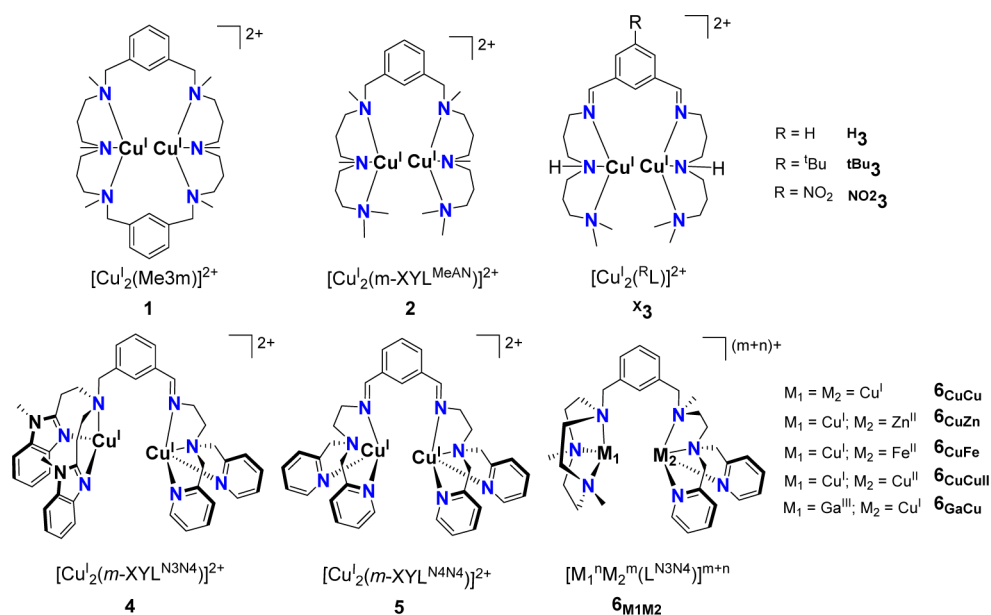
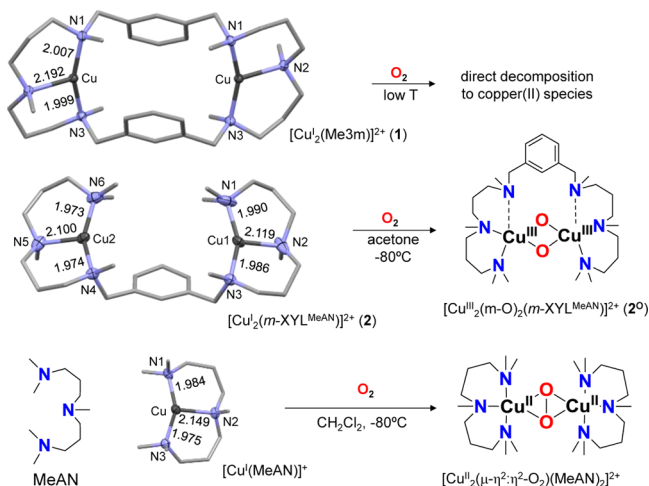


Figure 1. Dicopper and heterobimetallic complexes studied by our group.

### Scheme 2. Reactivity toward O<sub>2</sub> of the Structurally Related 1, 2, and [Cu<sup>I</sup>(MeAN)]<sup>+α</sup>



<sup>α</sup>Cu–N distances in Å are indicated in the X-ray crystal structures of the starting copper(I) complexes.

indicated that O<sub>2</sub> binding to H<sub>3</sub> was the fastest reported in the literature for a *meta*-xylyl bridged system ( $k = 3.8 \times 10^3 \text{ M}^{-1} \text{ s}^{-1}$  in acetone at  $-80 \text{ }^\circ\text{C}$ ).

Thus, the O<sub>2</sub> reactivity of this series of rather simple model systems shows that O<sub>2</sub>-binding at a dicopper site can overcome unfavorable O<sub>2</sub> binding at a monocopper site, provided Cu...Cu distance and first coordination sphere of the Cu ions exhibit enough flexibility to assemble the Cu<sub>2</sub>O<sub>2</sub> unit. In this line, it has been shown that the active site of tyrosinase is flexible and along its catalytic cycle it accommodates remarkable structural changes: the Cu...Cu distance varies from 4.9 to 2.9 Å and the geometry of the first coordination sphere switches from trigonal planar to five coordinate square pyramidal.<sup>4,24</sup>

### 2.2. O<sub>2</sub> Binding at Dicopper Unsymmetric Systems

Subsequently, the dioxygen chemistry of the unsymmetric complex [Cu<sub>2</sub><sup>I</sup>(*m*-XYL<sup>N3N4</sup>)<sup>2+</sup> (4, Figure 1) was studied.<sup>25</sup> The dinucleating ligand *m*-XYL<sup>N3N4</sup> was designed to bear two

different copper coordination sites. The first one offers a tricoordinating environment provided by two benzimidazole rings attached to an aliphatic nitrogen.<sup>26,27</sup> This is connected through a *meta*-xylyl moiety to a second site composed by two aliphatic amines and two pyridines giving a tetradentate environment.<sup>28</sup> Both donor sets had been previously reported and studied in Cu<sup>I</sup>/O<sub>2</sub> chemistry. Compound 4 was characterized by X-ray diffraction analysis, which showed one of the cuprous ions in a N<sub>3</sub> T-shaped geometry and the other lying in a N<sub>4</sub> distorted trigonal-pyramidal environment.

Acetone solutions of 4 were exposed to dioxygen ( $-90 \text{ }^\circ\text{C}$ ) to generate a metastable red-brown species with UV-vis features at 478 nm ( $\epsilon = 7.8 \text{ mM}^{-1} \text{ cm}^{-1}$ ) and a broad band centered at 600 nm (Figure 2b). Resonance Raman experiments showed two isotope-sensitive peaks at 832 cm<sup>-1</sup> ( $\Delta(^{18}\text{O}_2) = -45 \text{ cm}^{-1}$ ) and at 520 cm<sup>-1</sup> ( $\Delta(^{18}\text{O}_2) = -22 \text{ cm}^{-1}$ ), characteristic of O–O and Cu–O stretching vibrations of dicopper end-on *trans*-peroxo-dicopper(II) species (<sup>I</sup>P) with the general formula [Cu<sup>II</sup><sub>2</sub>(O<sub>2</sub>)(*m*-XYL<sup>N3N4</sup>)<sup>2+</sup> (4<sup>TP</sup>).<sup>9,29</sup> The symmetric analogue bearing two tetradentate binding sites [Cu<sub>2</sub><sup>I</sup>(*m*-XYL<sup>N4N4</sup>)<sup>2+</sup> (5, Figure 1) reacted with O<sub>2</sub> in acetone at  $-90 \text{ }^\circ\text{C}$  to form a metastable purple compound with intense UV/vis bands at  $\lambda_{\text{max}} = 500 \text{ nm}$  ( $\epsilon = 5 \text{ mM}^{-1} \text{ cm}^{-1}$ ) and 635 nm ( $\epsilon = 3.3 \text{ mM}^{-1} \text{ cm}^{-1}$ ), typical of a *trans*-peroxo species (<sup>S</sup>TP). Despite sharing the same O<sub>2</sub> coordination mode and having similar spectroscopic features, 4<sup>TP</sup> and 5<sup>TP</sup> present markedly different reactivity toward substrates (see section 3).

### 2.3. Heterobimetallic Systems

Following the use of ligand *m*-XYL<sup>N3N4</sup> to prepare unsymmetric Cu<sub>2</sub>O<sub>2</sub> species, we targeted the preparation of an unsymmetric dinucleating polyamine ligand, L<sup>N3N4</sup> (Scheme 3), specially designed to accommodate two metals in markedly different coordination environments.<sup>30</sup> In this case, the tridentate site is constituted by a triazacyclononane ring (N<sub>3</sub>)<sup>31</sup> and a *meta*-xylyl linker connects it to a tetradentate moiety (N<sub>4</sub>).<sup>28</sup> With this new ligand in hand, not only the homodimetallic dicopper(I) complex was prepared, but also a set of heterodimetallic complexes combining copper(I) and another metal. Although O<sub>2</sub> binding took place, the reaction occurred intermolecularly forming symmetric Cu<sub>2</sub>O<sub>2</sub> species (Scheme 3).

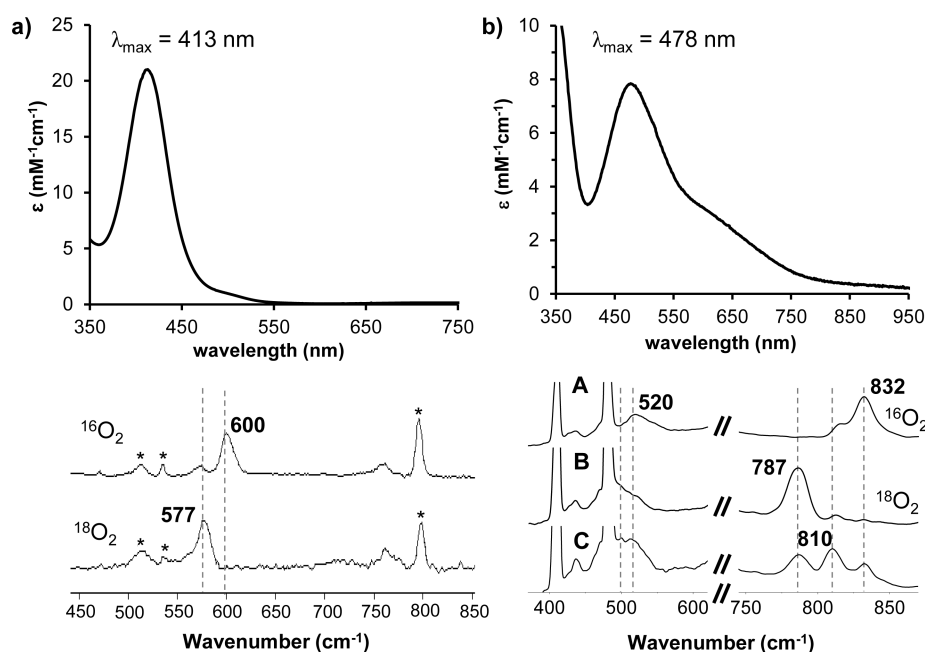
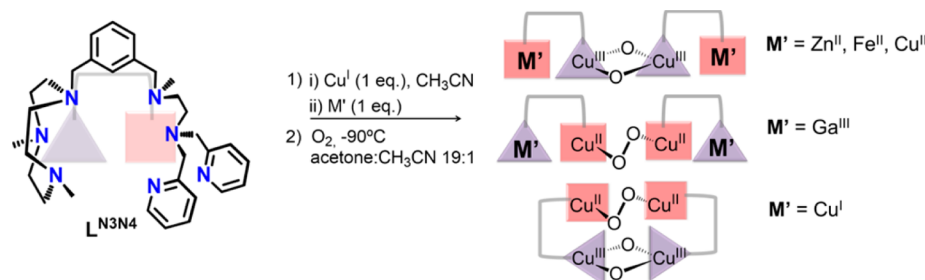


**Figure 2.** (a) UV–vis spectrum (top) and resonance Raman (bottom) of  $2^{\text{O}}$  generated in acetone at  $-90$  °C with  $^{16}\text{O}_2$  and  $^{18}\text{O}_2$  (laser excitation at 413 nm). (b) UV–vis spectrum (top) and resonance Raman (laser excitation at 488 nm) of  $4^{\text{TP}}$  generated in acetone at  $-90$  °C with  $^{16}\text{O}_2$  (A),  $^{18}\text{O}_2$  (B), and  $^{18}\text{O}^{16}\text{O}$  (C).

### Scheme 3. Homodimetallic and Heterodimetallic Species Generated Using $\text{L}^{\text{N}_3\text{N}_4}$



Reaction of  $[\text{Cu}^{\text{I}}(\text{L}^{\text{N}_3\text{N}_4})]^{2+}$  ( $6_{\text{CuCu}}$ , Figure 1) with  $\text{O}_2$  in an acetonitrile:acetone 1:19 mixture at  $-90$  °C was monitored by UV–vis spectroscopy and the fast formation of two bands at 530 nm ( $\epsilon = 2 \text{ mM}^{-1} \text{ cm}^{-1}$ ) and 405 nm ( $\epsilon = 15 \text{ mM}^{-1} \text{ cm}^{-1}$ ) was observed (Figure 3a). While the former band decayed, the second one was stable under these conditions. The different time evolution of these bands indicated that they correspond to two different  $\text{Cu}_2\text{O}_2$  species. Initial assignment was done by comparison with the reactivity of monomeric copper(I) complexes. On the one hand,  $[\text{Cu}^{\text{I}}(\text{Me}_3\text{tacn})]^+$  ( $\text{Me}_3\text{tacn} = 1,4,7$ -trimethyl-1,4,7-triazacyclononane) affords  $\text{O}$  species upon reaction with  $\text{O}_2$  at low temperatures with UV–vis features at 307 nm ( $16 \text{ mM}^{-1} \text{ cm}^{-1}$ ) and 412 nm ( $18 \text{ mM}^{-1} \text{ cm}^{-1}$ ).<sup>32</sup> On the other hand,  $[\text{Cu}^{\text{I}}(\text{uns-penp})]^+$  ( $\text{uns-penp} = (2\text{-aminoethyl})\text{-bis}(2\text{-pyridylmethyl})\text{amine}$ ) is reported to generate  $^{\text{T}}\text{P}$  species with a characteristic band at  $\lambda_{\text{max}} = 535$  nm upon reaction with  $\text{O}_2$ .<sup>28</sup> Thus, we speculated that a dimeric species derived from the interaction of two  $6_{\text{CuCu}}$  molecules was formed. The  $\text{O}$  core arose from the interaction between two copper centers in the  $\text{N}_3$  site, while the  $^{\text{T}}\text{P}$  species corresponded to the interaction of two copper atoms in the  $\text{N}_4$  site. Further evidence for this intermolecular oxygen binding emerged from cryospray ionization

mass experiments (CSI-MS) at  $-90$  °C that showed a dominant peak with a mass value and isotopic pattern fully consistent with the proposed dimeric species (Figure 3a, inset).

After studying the reactivity of  $6_{\text{CuCu}}$  toward  $\text{O}_2$  we aimed at synthesizing heterodimetallic complexes. In order to do so,  $\text{Cu}^{\text{I}}$  (1 equiv) and another metal such as  $\text{Zn}^{\text{II}}$ ,  $\text{Fe}^{\text{II}}$ ,  $\text{Cu}^{\text{II}}$  or  $\text{Ga}^{\text{III}}$  (1 equiv) were added sequentially to  $\text{L}^{\text{N}_3\text{N}_4}$  under an anaerobic atmosphere. Analysis of the different complexes by NMR and MS techniques showed that  $\text{L}^{\text{N}_3\text{N}_4}$  selectively held two different metals, so that pure heterodimetallic complexes with the general formula  $[\text{Cu}^{\text{I}}\text{M}^{\text{n}}(\text{L}^{\text{N}_3\text{N}_4})]^{n+1}$  ( $6_{\text{CuM}}$  or  $6_{\text{MCu}}$ ) were obtained. Further evidence about the heterobimetallic character of these complexes was gained through studying their reactivity toward  $\text{O}_2$ . Complexes containing  $\text{Cu}^{\text{I}}$  and a divalent complementary metal such as  $\text{Zn}^{\text{II}}$ ,  $\text{Cu}^{\text{II}}$  or  $\text{Fe}^{\text{II}}$  formed exclusively  $\text{O}$  species, suggesting that  $\text{Cu}^{\text{I}}$  was exclusively located at the tacn site (Figure 3b top). In sharp contrast, the use of a trivalent metal such as  $\text{Ga}^{\text{III}}$  led to the exclusive formation of  $^{\text{T}}\text{P}$  species and no formation of  $\text{O}$  species was detected (Figure 3b bottom). This was an indication that  $\text{Cu}^{\text{I}}$  resided in the tetradentate site. Thus, depending on the complementary metal,  $\text{L}^{\text{N}_3\text{N}_4}$  was able to locate the copper(I) center in one of the binding sites or the other.



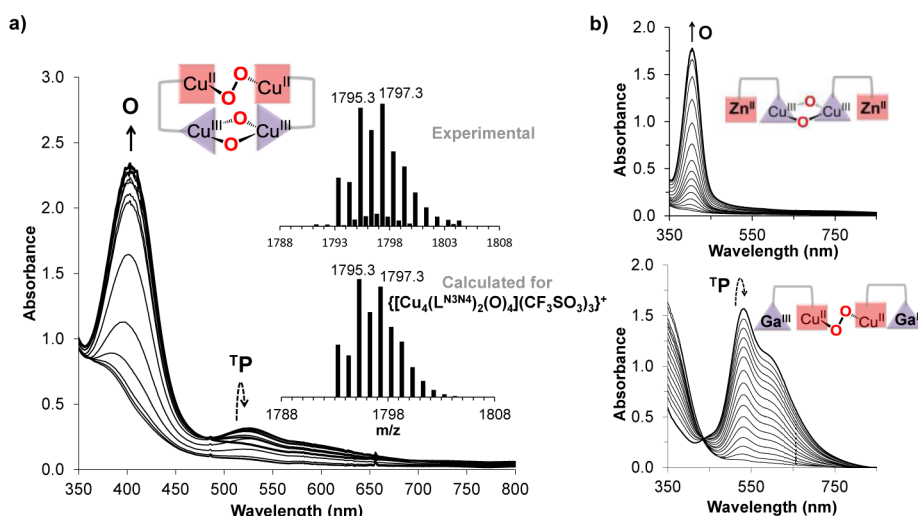


**Figure 3.** (a) Formation of **O** and **<sup>TP</sup>** species upon reaction of  $6_{\text{CuCu}}$  (0.3 mM) with  $\text{O}_2$  at  $-90^\circ\text{C}$ . Inset: CSI-MS spectra at  $-90^\circ\text{C}$  for the reaction of  $6_{\text{CuCu}}$  with  $\text{O}_2$  to form dimeric species. (b) Top: formation of **O** species upon reaction of  $6_{\text{CuZn}}$  (0.3 mM) with  $\text{O}_2$  at  $-90^\circ\text{C}$ . Bottom: formation of **<sup>TP</sup>** species upon reaction of  $6_{\text{GaCu}}$  (0.79 mM) with  $\text{O}_2$  at  $-90^\circ\text{C}$ .

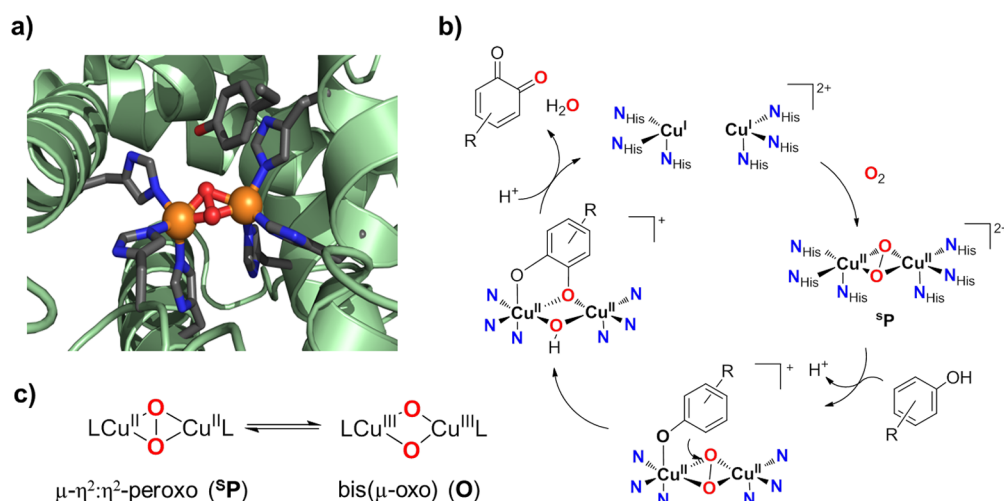


**Figure 4.** (a) X-ray structure of substrate-bound tyrosinase (1WX2.pdb).<sup>24</sup> (b) Mechanism of action of tyrosinase toward the hydroxylation of a monophenolic substrate. (c) Equilibrium between bis( $\mu$ -oxo) (**O**) and  $\mu$ - $\eta^2$ : $\eta^2$ -peroxo (**<sup>S<sup>P</sup></sup>**) complexes.

### 3. REPRODUCING TYROSINASE ACTIVITY

Mimicking the structure and reactivity of tyrosinase with model compounds is a topic of major interest in synthetic bioinorganic chemistry. This enzyme catalyzes the *ortho*-hydroxylation of phenols to catechols and the two electron oxidation of the latter to quinones. Besides its biological relevance,<sup>33</sup> the reaction is remarkable because of its *ortho*-regioselectivity, which is difficult to obtain with nonenzymatic synthetic methodologies.<sup>34</sup> In addition, this is also a very unique reaction from the perspective of  $\text{O}_2$  activation, since a full catalytic cycle involves a  $4e^-$  oxidation of the substrate with full reduction of a single  $\text{O}_2$  molecule. The active site of tyrosinase contains two copper centers where each copper ion is coordinated by three histidine residues.<sup>24</sup> The *deoxy* form of tyrosinase consists in a dicopper(I) active site, that upon reaction with  $\text{O}_2$  forms a **<sup>S<sup>P</sup></sup>** species (Figure 4a). In subsequent steps, the phenolic substrate (in its phenolate form) coordinates to the  $\text{Cu}_2\text{O}_2$  core, and *ortho*-hydroxylation occurs via an electrophilic attack of the peroxide over the aromatic ring of the phenolic substrate giving rise to the formation of the corresponding catechol (Figure 4b).

Further  $2e^-$  oxidation to quinone regenerates the *deoxy* resting state.

Through the use of model systems, Tolman and co-workers demonstrated the existence of a reversible O–O bond cleavage so that **O** and **<sup>S<sup>P</sup></sup>** isomers can be in equilibrium (Figure 4c).<sup>35</sup> This observation calls into question which of the two isomers is the actual executor of the hydroxylation in tyrosinase. Indeed, several works with model systems have demonstrated that the **O** isomer, despite not being detected in biological systems, is also competent for performing the *ortho*-hydroxylation of exogenous phenolates to give catechols.<sup>11,36</sup>

Given the similarity between the coordination environment of copper(I) in **2** and tyrosinase, we explored the ability of **2<sup>O</sup>** to perform the *ortho*-hydroxylation of phenols.<sup>37</sup> Reaction of **2<sup>O</sup>** with 10 equiv of sodium *para*-chlorophenolate (*p*-Cl-C<sub>6</sub>H<sub>4</sub>ONa) afforded the corresponding 4-chlorocatechol in 67% yield with respect to the initial dicopper complex. Moreover, an immediate color change from bright yellow to purple was observed when **2<sup>O</sup>** reacted with this phenolate at  $-90^\circ\text{C}$ . rRaman provided direct evidence that this chromophore arose

from phenolate binding to the bis( $\mu$ -oxo)dicopper(III) core ( $2^{\text{O}}$ -OC<sub>6</sub>H<sub>4</sub>Cl).

A series of analogous species were generated by reaction of  $2^{\text{O}}$  with 1.5 equiv of sodium *para*-substituted-phenolates (X = F, CO<sub>2</sub>CH<sub>3</sub>, Cl, CN) and the plot of the decay rates against the corresponding Hammett parameter ( $\sigma^+$ ) afforded a linear correlation with a negative slope indicative of an electrophilic oxidizing species that attacks the aromatic ring. Using a similar experimental procedure, tyrosinase and some of its functional model systems had already exhibited a similar electrophilic behavior.<sup>26,27,36,38,39</sup>

Apart from  $2^{\text{O}}$ , other Cu<sub>2</sub>O<sub>2</sub> complexes featuring a **O** species have been reported to behave as tyrosinase functional models. O–O bond cleavage upon phenolate coordination was observed for the <sup>5</sup>P hydroxylating species [Cu<sup>II</sup><sub>2</sub>(O<sub>2</sub>)(DBED)]<sup>2+</sup> prior to aromatic attack<sup>36</sup> and analogously to  $2^{\text{O}}$ , a **O** species was detected in [Cu<sup>III</sup><sub>2</sub>(O)<sub>2</sub>(L<sup>AG</sup>)<sub>2</sub>]<sup>2+</sup> before phenolate addition<sup>40</sup> (Figure 5).

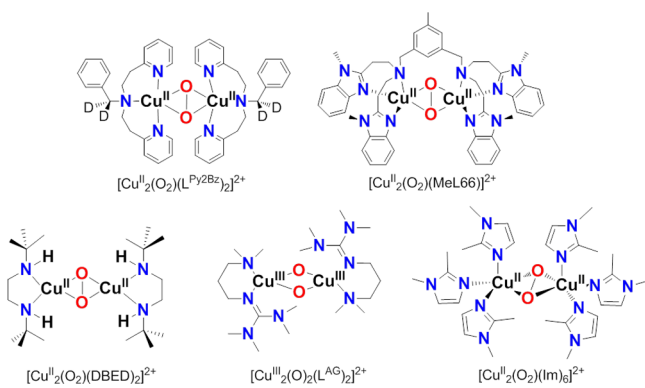


**Figure 5.** Spectroscopically trapped Cu<sub>2</sub>O<sub>2</sub> systems that act as functional tyrosinase models.

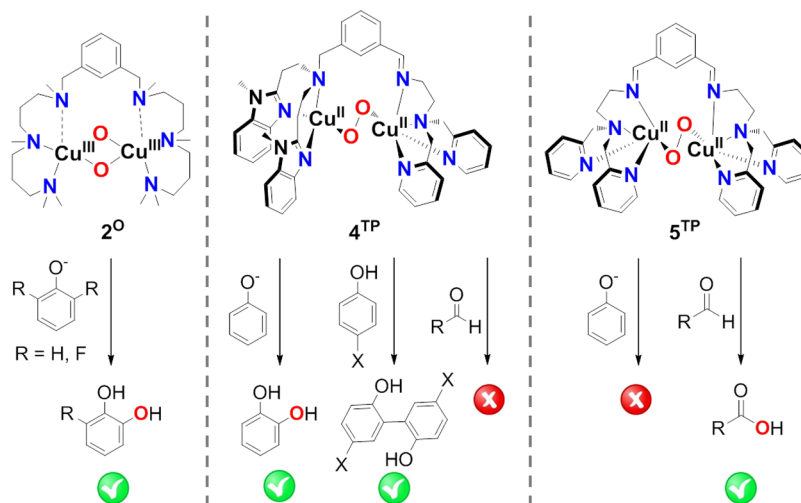
On the other hand, <sup>5</sup>P species were observed in the phenolate *ortho*-hydroxylation carried out by [Cu<sup>II</sup><sub>2</sub>(O<sub>2</sub>)(L<sup>Py2Bz</sup>)<sub>2</sub>]<sup>2+</sup>, [Cu<sup>II</sup><sub>2</sub>(O<sub>2</sub>)(MeL66)]<sup>2+</sup>, and [Cu<sup>II</sup><sub>2</sub>(O<sub>2</sub>)(Im)<sub>6</sub>]<sup>2+</sup> (Figure 5).<sup>26,39,41</sup> Interestingly, reaction of [Cu<sup>III</sup><sub>2</sub>(O)<sub>2</sub>(L<sup>AG</sup>)<sub>2</sub>]<sup>2+</sup>, [Cu<sup>II</sup><sub>2</sub>(O<sub>2</sub>)(L<sup>Py2Bz</sup>)<sub>2</sub>]<sup>2+</sup>, [Cu<sup>II</sup><sub>2</sub>(O<sub>2</sub>)(MeL66)]<sup>2+</sup>, and [Cu<sup>II</sup><sub>2</sub>(O<sub>2</sub>)(Im)<sub>6</sub>]<sup>2+</sup> with phenolates did not show formation of any adduct derived from the interaction between copper and phenolate. Instead, direct bleaching of the spectroscopic features of the Cu<sub>2</sub>O<sub>2</sub>

species was observed concomitant with formation of the catechol product. Overall,  $2^{\text{O}}$  turned out to be the first Cu<sub>2</sub>O<sub>2</sub> system that could reproduce tyrosinase reactivity through a **O** species that could be detected before and after phenolate coordination.

We also explored the reactivity of the unsymmetric  $4^{\text{TP}}$  toward external substrates.<sup>25</sup> This species showed nucleophilic character, characteristic of <sup>T</sup>P species. For example, it reacted with strong acids to release H<sub>2</sub>O<sub>2</sub> and dicopper(II), while reaction with PPh<sub>3</sub> caused dioxygen liberation and formation of the dicopper(I)-PPh<sub>3</sub> complex. Strikingly,  $4^{\text{TP}}$  also reacted when exposed to *para*-substituted sodium phenolates, leading to the formation of the corresponding catechol products (Scheme 4). Detailed kinetic analysis of the reaction provided evidence for a two-step reaction mechanism, where an initial reversible phenolate coordination process was followed by the attack of the Cu<sub>2</sub>O<sub>2</sub> center to the substrate during the rate-determining step. A Hammett plot provided a  $\rho$  value of  $-2.2$ , suggesting that the Cu<sub>2</sub>O<sub>2</sub> center was acting as an electrophilic oxidant. An inverse kinetic isotopic effect (KIE = 0.88), consistent with sp<sup>2</sup> to sp<sup>3</sup> isomerization, also pointed toward the proposed mechanistic scenario.<sup>42</sup> The reactivity of  $4^{\text{TP}}$  against phenols was also explored.<sup>42</sup> In this case, the substrate did not suffer *ortho*-hydroxylation and instead the reaction led to 1e<sup>-</sup>/1H<sup>+</sup> oxidation, affording the C–C coupling products (Scheme 4). Thermodynamic and activation parameters for the two-step phenolate *ortho*-hydroxylation were also determined and they correlated well with the computed values of the electrophilic attack of the <sup>T</sup>P moiety over the aromatic ring.<sup>25</sup> Computational studies also provided evidence that coordination of the phenolate was occurring in the copper atom located in the less hindered N<sub>3</sub> site, so that the peroxide moiety and the arene ring lay in a proper distance and orientation to elicit successful electrophilic attack. Presumably the unsymmetrical design of the dinucleating ligand *m*-XYL<sup>N3N4</sup> was essential to lead, for the first time, to a <sup>T</sup>P species capable of performing electrophilic aromatic hydroxylation of phenolates.

In sharp contrast to the reactivity offered by the unsymmetric  $4^{\text{TP}}$  species, the symmetric analogue  $5^{\text{TP}}$  presented a reactivity similar to that previously described for other <sup>T</sup>P compounds. Thus,  $5^{\text{TP}}$  behaved as a nucleophile and it reacted with benzaldehydes to form the corresponding benzoic acid in quantitative yields. However, only bleaching of the  $5^{\text{TP}}$  spectroscopic features was observed upon addition of sodium

**Scheme 4.** Reaction of  $2^{\text{O}}$ ,  $4^{\text{TP}}$ , and  $5^{\text{TP}}$  toward Substrates



*para*-chlorophenolate without formation of the *ortho*-hydroxylated product (Scheme 4).

Very recently, Solomon et al. described the first example of a  $^1\text{P}$ -type species that led to a  $\text{O}$ -type species by  $\text{O}-\text{O}$  cleavage,<sup>43</sup> a process that had been previously observed only for  $^5\text{P}$  species.<sup>31</sup> Based on these experimental observations and with new calibrated DFT calculations, the same authors proposed that  $4^{\text{TP}}$  was not the electrophile in the *ortho*-hydroxylation of phenolates, but instead coordination of the substrate led to  $\text{O}-\text{O}$  cleavage to generate an  $\text{O}$ -type species prior to arene attack. Further spectroscopic studies on the characterization of the  $\text{Cu}_2\text{O}_2$  species generated after phenolate coordination to  $4^{\text{TP}}$  may be necessary to establish whether  $\text{O}-\text{O}$  cleavage occurs prior or after electrophilic aromatic attack.

Few synthetic models of tyrosinase achieve significant catalytic phenol hydroxylation using oxygen. Réglér et al.<sup>44</sup> and Tuzek et al.<sup>45</sup> reported the first catalytic tyrosinase models, which were able to *ortho*-hydroxylate 2,4-di-*tert*-butylphenol in the presence of a copper(I) complex,  $\text{O}_2$ , and excess  $\text{NEt}_3$ , giving  $\sim 16$  TN (TN = turnover number) of 3,5-di-*tert*-butyl-*o*-quinone. The active oxygenated species responsible for the observed chemistry were not identified, and the reactions fall short in terms of synthetic value. Interestingly, recent reports by Herres-Pawlis et al. and Lumb et al. have shown catalytic *ortho*-hydroxylation of a wide variety of phenols using  $\text{O}_2$  as oxidant and Cu-polyamine complexes as catalysts, in reactions with potential synthetic value.<sup>46–48</sup>

#### 4. NOVEL REACTIVITY: C–F BOND DEFLUORINATION HYDROXYLATION

After studying the *ortho*-hydroxylation of phenolates by  $2^{\text{O}}$ , we speculated if this compound could be able to cleave a *ortho* carbon–fluorine bond of a fluorophenolate. C–F bonds are the strongest single bond to carbon (stronger than C–H) and they are considered the most inert functionalities due to their high bond dissociation energy of  $130 \text{ kcal mol}^{-1}$ .<sup>49</sup> Accordingly, in spite of binding the active site of tyrosinase, 2-fluorophenolates cannot be further hydroxylated and they are considered enzyme inhibitors.<sup>50</sup>

To our surprise, reaction of  $2^{\text{O}}$  with 3 equiv of sodium 2,6-difluorophenolate ( $\text{NaOC}_6\text{H}_3\text{F}_2$ ) at  $-90^\circ\text{C}$  in acetone showed the immediate decay of the spectroscopic features associated with  $\text{O}$  and the formation of a purple species with  $\lambda_{\text{max}}$  at 520 nm, that was unstable and decayed within 5 min (Figure 6).<sup>51</sup> Despite its thermal instability, CSI-MS experiments at  $-90^\circ\text{C}$  showed a very clean spectrum featuring a major peak corresponding to  $2^{\text{O}}$  and a secondary one at  $m/z = 765.3194$ , fully consistent with phenolate coordinated to the  $\text{O}$  core in  $2^{\text{O}}$  ( $2^{\text{O}}\text{-OC}_6\text{H}_3\text{F}_2$ ) (Figure 6, inset). MS-MS tandem experiments on this peak showed the loss of one phenolate unit demonstrating that substrate had not been yet hydroxylated at this stage.

$^1\text{H}$  NMR and HPLC analysis after  $2^{\text{O}}\text{-OC}_6\text{H}_3\text{F}_2$  decomposition indicated the formation of 3-fluorocatechol in 21% yield with respect to  $2^{\text{O}}$ . Thus, cleavage of the *ortho* C–F bond had taken place to obtain the *ortho*-hydroxylated-defluorinated product. Importantly, 82% of  $^{18}\text{O}$ -labeled catechol product was obtained when  $^{18}\text{O}_2$  was used in the generation of  $2^{\text{O}}$ , indicating that the C–F bond was cleaved by the bis( $\mu$ -oxo) unit. 4-substituted 2-fluorophenolates were used to draw a Hammett plot by fitting the decay of the phenolate-bound  $2^{\text{O}}$ . A negative slope ( $\rho = -2.4$ ) was obtained, indicating that the reaction occurred via an electrophilic attack on the aromatic ring of the phenolate, analogously to the thoroughly studied phenolate

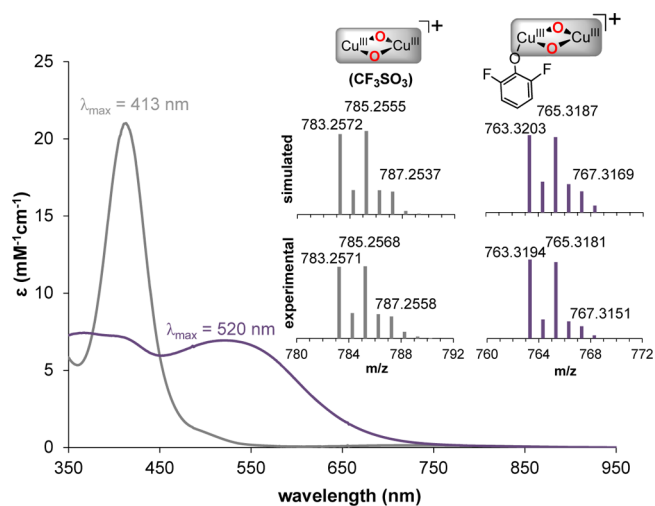
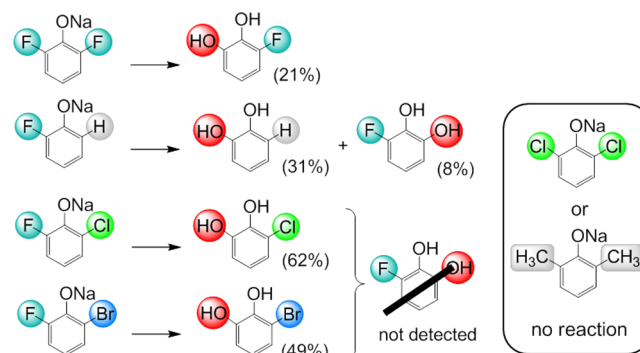


**Figure 6.** UV-vis spectra of  $2^{\text{O}}$  (gray) and  $2^{\text{O}}\text{-OC}_6\text{H}_3\text{F}_2$  (purple) formed after the addition of 3 equiv sodium 2,6-difluorophenolate in acetone at  $-90^\circ\text{C}$ . Inset: CSI-MS spectrum of  $2^{\text{O}}$  and  $2^{\text{O}}\text{-OC}_6\text{H}_3\text{F}_2$  at  $-90^\circ\text{C}$ .

*ortho*-hydroxylation. Furthermore, the *ortho*-hydroxylation-defluorination reaction was regioselective for the *ortho* position: reaction with 4-fluorophenolate afforded only 4-fluorocatechol. More interestingly, an exquisite chemoselectivity for the C–F bond was observed when unsymmetric phenolates bearing one fluorine and a different halogen (Cl or Br) in the *ortho* positions were used as substrates (Scheme 5). We reasoned that once

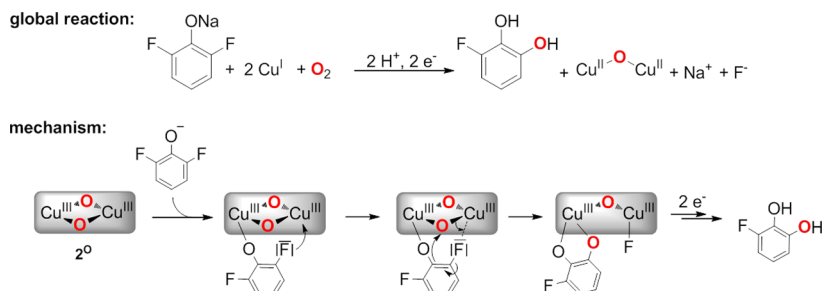
#### Scheme 5. Selective *ortho*-Hydroxylation–Defluorination Reactions Promoted by $2^{\text{O}}$



<sup>a</sup>Reaction conditions: (i)  $2^{\text{O}}$ , sodium phenolate (3 equiv), acetone,  $-90^\circ\text{C}$ ; (ii) acidic workup.

phenolate binds to a copper center in  $2^{\text{O}}$ , an interaction of the F atom of the substrate to the adjacent Cu ion may be key to lock the orientation of the arene ring, leading to selective hydroxylation (Scheme 6).

Interestingly, we found that this *ortho*-hydroxylation-defluorination reaction was not exclusive of  $2^{\text{O}}$ . Following the same procedure as for  $2^{\text{O}}$ ,  $\text{NaOC}_6\text{H}_3\text{F}_2$  was added to the preformed  $^5\text{P}$  species derived from  $[\text{Cu}^{\text{I}}(\text{DBED})]^+$  and  $[\text{Cu}^{\text{I}}(\text{L}^{\text{Py}2\text{Bz}})]^+$  (Figure 5). Interestingly, while the DBED-based system afforded 23% of 3-fluorocatechol product,  $\text{L}^{\text{Py}2\text{Bz}}$ -based complex only afforded trace amounts. As explained in section 3,  $^5\text{P}$  species derived from  $[\text{Cu}^{\text{I}}(\text{DBED})]^+$  suffers  $\text{O}-\text{O}$  bond cleavage to give  $\text{O}$  species once phenolate binding occurs.<sup>36</sup> Thus, the presence of a  $\text{O}$  core after phenolate binding seems to be key for the success of the C–F bond cleavage.

Scheme 6<sup>a</sup>

<sup>a</sup>Top: Balanced equation for the defluorination reaction carried out by **2**. Bottom: Proposed mechanism of *ortho*-hydroxylation-defluorination of 2-fluorophenolates by **2**<sup>o</sup>.

One of the main handicaps that we found while progressing in the work was the low yield of the *ortho*-hydroxylation-defluorination products. Although there is no neat gain or loss of electrons along this organic transformation (Scheme 6), a change in the copper oxidation state from +3 to +2 is observed experimentally at the end of the reaction. In the absence of a reducing agent, the reducing electrons may originate from preformed  $\text{Cu}_2\text{O}_2$  molecules, which may liberate electrons by reversible  $\text{O}_2$  binding. This would largely limit reaction yields because half of the starting  $\text{Cu}_2\text{O}_2$  molecules would act as simple reductants. To corroborate this hypothesis the use of an external reducing agent as the source of electrons was envisioned. While in the case of **2**<sup>o</sup> the presence of reductant caused its immediate decomposition,<sup>40</sup> addition of sodium ascorbate in the reaction of  $[\text{Cu}^{\text{II}}_2(\text{O}_2)(\text{DBED})_2]$  with sodium 2-chloro-6-fluorophenolate or 2-bromo-6-fluorophenolate raised the yields of 3-chlorocatechol or 3-bromocatechol from 34% and 41% respectively to 83% in both cases.

## 5. CONCLUDING REMARKS

In conclusion, along our work we have observed that flexible ligand scaffolds that permit synergistic cooperation in  $\text{O}_2$  binding constitute a valuable strategy to prepare well-defined  $\text{Cu}_2\text{O}_2$  species with symmetric and unsymmetric environments. With these molecules in hand, basic aspects of the reactivity of tyrosinase, including its remarkable regioselectivity, could be reproduced. Controlled cleavage of the O–O bond also allowed to perform hydroxylation of more inert functionalities such as fluorophenolates. Translation of this stoichiometric reactivity into catalytic processes is an interesting future goal in order to make them valuable in synthetic chemistry. Introduction of unsymmetry on the  $\text{Cu}_2\text{O}_2$  core has also shown to uncover novel reactivities not attained with symmetric analogues. Finally, ligand design has also allowed the preparation of  $\text{O}_2$  activating heterometallic complexes where site specific metalation can be accomplished.

Undoubtedly, one of the most interesting aspects to be addressed by future work in this field of research is the development of heterometallic systems that enable the preparation of heterometallic dioxygen adducts. It can be envisioned that these novel molecules will provide novel reactivities and selectivities. Presumably, careful design of highly preorganized ligand scaffolds may be necessary in order to prevent competitive intermolecular  $\text{O}_2$  binding that lead to homometallic cores, although some degree of intramolecular flexibility will still be needed in order to facilitate bimetallic  $\text{O}_2$  binding. On the other hand, the discovery of a dicopper active site in particular methane monooxygenase<sup>52</sup> has raised the question about the

nature of the oxidizing species responsible for the oxidation of methane in this enzyme.  $\text{Cu}_2\text{O}_2$  species are likely candidates, but they must have a different nature from any of the copper-dioxygen species discovered so far, because none have shown the ability of oxidizing strong alkyl C–H bonds. Synthetic bioinorganic chemistry must provide lessons to understand the nature of the species involved in this challenging reaction, and the specific paths by which the  $\text{O}_2$  molecule is activated to engage in this endeavor.

## AUTHOR INFORMATION

### Corresponding Authors

\*E-mail: [anna.company@udg.edu](mailto:anna.company@udg.edu).

\*E-mail: [miquel.costas@udg.edu](mailto:miquel.costas@udg.edu).

### Notes

The authors declare no competing financial interest.

### Biographies

**Joan Serrano-Plana** received his bachelor in Chemistry from the University of Girona (UdG) in 2012. Thereafter he joined the group of Dr. Costas, obtaining his Master degree in 2013. He is currently a Ph.D. student in the same group. His interests are based on copper and non-heme iron model systems for substrate oxidation.

**Isaac Garcia-Bosch** received his Ph.D. in Chemistry from UdG in 2011. After his postdoctoral studies under the mentorship of Prof. Karlin (Johns Hopkins University, Baltimore), in 2015, he was appointed as an Assistant Professor in the Department of Chemistry at the Southern Methodist University (Dallas). His research is focused on the development of first row metal complexes for  $\text{O}_2$  reduction,  $\text{H}_2\text{O}$  oxidation and bioinspired synthetic catalysis.

**Anna Company** received her Ph.D. in Chemistry at UdG in 2008. After postdoctoral studies in the group of Prof. Driess at the Technische Universität Berlin (Germany), in 2011, she moved back to UdG, where she is currently appointed as a RyC fellow. Her research interests include activation of small molecules using first row transition metal complexes.

**Miquel Costas** (Ph.D. in Chemistry 1999, UdG) is professor of Chemistry at the UdG. After postdoctoral studies at the University of Minnesota with Prof. Que, he returned to Spain as a RyC fellow in 2002. Since 2006, he has been group leader of the QBIS-CAT research group. His research interests cover synthetic bioinorganic chemistry, and bioinspired catalysis.

## ACKNOWLEDGMENTS

Support from the European Commission (ERC-2009-StG-239910 to M.C., 2011-CIG-303522 to A.C., and Marie Curie IOF to I.G.-B.), the Spanish Ministry of Science (CTQ2012-



37420-C02-01/BQU to M.C., CSD2010-00065 to M.C., and RyC contract to A.C.) and Generalitat de Catalunya (ICREA Academia Award to M.C.) is acknowledged.

## REFERENCES

- (1) Bäckvall, J.-E. *Modern Oxidation Methods*; Wiley-VCH Verlag GmbH: Weinheim, 2004.
- (2) Sawyer, D. T. *Oxygen Chemistry*; Oxford University Press: New York, 1991.
- (3) Bertini, I.; Gray, H. B.; Stiefel, E. I.; Valentine, S. J. *Biological Inorganic Chemistry: Structure and Reactivity*; University Science Books: Sausalito, CA, 2007.
- (4) Solomon, E. I.; Heppner, D. E.; Johnston, E. M.; Ginsbach, J. W.; Cirera, J.; Qayyum, M.; Kieber-Emmons, M. T.; Kjaergaard, C. H.; Hadt, R. G.; Tian, L. Copper Active Sites in Biology. *Chem. Rev.* **2014**, *114*, 3659–3853.
- (5) Shi, Z.; Zhang, C.; Tang, C.; Jiao, N. Recent advances in transition-metal catalyzed reactions using molecular oxygen as the oxidant. *Chem. Soc. Rev.* **2012**, *41*, 3381–3430.
- (6) Wendlandt, A. E.; Suess, A. M.; Stahl, S. S. Copper-Catalyzed Aerobic Oxidative C-H Functionalizations: Trends and Mechanistic Insights. *Angew. Chem., Int. Ed.* **2011**, *50*, 11062–11087.
- (7) Bento, I.; Carrondo, M. A.; Lindley, P. F. Reduction of dioxygen by enzymes containing copper. *JBC, J. Biol. Inorg. Chem.* **2006**, *11*, 539–547.
- (8) Swiegers, G. *Bioinspiration and Biomimicry in Chemistry*; John Wiley & Sons Inc.: Hoboken, NJ, 2012.
- (9) Mirica, L. M.; Ottenwaelder, X.; Stack, T. D. P. Structure and Spectroscopy of Copper–Dioxygen Complexes. *Chem. Rev.* **2004**, *104*, 1013–1046.
- (10) Lewis, E. A.; Tolman, W. B. Reactivity of Dioxygen–Copper Systems. *Chem. Rev.* **2004**, *104*, 1047–1076.
- (11) Rolff, M.; Schottenheim, J.; Decker, H.; Tuzek, F. Copper–O<sub>2</sub> reactivity of tyrosinase models towards external monophenolic substrates: molecular mechanism and comparison with the enzyme. *Chem. Soc. Rev.* **2011**, *40*, 4077–4098.
- (12) Chufán, E. E.; Puii, S. C.; Karlin, K. D. Heme–Copper/Dioxygen Adduct Formation, Properties, and Reactivity. *Acc. Chem. Res.* **2007**, *40*, 563–572.
- (13) Haack, P.; Limberg, C. Molecular CuII–O–CuII Complexes: Still Waters Run Deep. *Angew. Chem., Int. Ed.* **2014**, *53*, 4282–4293.
- (14) Garcia-Bosch, I.; Ribas, X.; Costas, M. Well-Defined Heterometallic and Unsymmetric M<sub>2</sub>O<sub>2</sub> Complexes Arising from Binding and Activation of O<sub>2</sub>. *Eur. J. Inorg. Chem.* **2012**, *2012*, 179–187.
- (15) Bulkowski, J. E.; Burk, P. L.; Ludmann, M.-F.; Osborn, J. A. Two-metal-substrate interactions: the reversible reaction of a Cu...Cu complex with CO and O<sub>2</sub>. *J. Chem. Soc., Chem. Commun.* **1977**, 498–499.
- (16) Karlin, K. D.; Nasir, M. S.; Cohen, B. I.; Cruse, R. W.; Kaderli, S.; Zuberbuehler, A. D. Reversible Dioxygen Binding and Aromatic Hydroxylation in O<sub>2</sub>-Reactions with Substituted Xylyl Dinuclear Copper(I) Complexes: Syntheses and Low-Temperature Kinetic/Thermodynamic and Spectroscopic Investigations of a Copper Monooxygenase Model System. *J. Am. Chem. Soc.* **1994**, *116*, 1324–1336.
- (17) Casella, L.; Carugo, O.; Gullotti, M.; Garofani, S.; Zanello, P. Hemocyanin and tyrosinase models. Synthesis, azide binding, and electrochemistry of dinuclear copper(II) complexes with poly-(benzimidazole) ligands modeling the met forms of the proteins. *Inorg. Chem.* **1993**, *32*, 2056–2067.
- (18) Ghosh, D.; Mukherjee, R. Modeling Tyrosinase Monooxygenase Activity. Spectroscopic and Magnetic Investigations of Products Due to Reactions between Copper(I) Complexes of Xylyl-Based Dinucleating Ligands and Dioxygen: Aromatic Ring Hydroxylation and Irreversible Oxidation Products. *Inorg. Chem.* **1998**, *37*, 6597–6605.
- (19) Company, A.; Lamata, D.; Poater, A.; Sola, M.; Rybak-Akimova, E. V.; Que, L.; Fontrodona, X.; Parella, T.; Llobet, A.; Costas, M. O<sub>2</sub> chemistry of dicopper complexes with alkyltriamine ligands. Comparing synergistic effects on O<sub>2</sub> binding. *Inorg. Chem.* **2006**, *45*, 5239–5241.
- (20) Liang, H.-C.; Zhang, C. X.; Henson, M. J.; Sommer, R. D.; Hatwell, K. R.; Kaderli, S.; Zuberbuehler, A. D.; Rheingold, A. L.; Solomon, E. I.; Karlin, K. D. Contrasting Copper–Dioxygen Chemistry Arising from Alike Tridentate Alkyltriamine Copper(I) Complexes. *J. Am. Chem. Soc.* **2002**, *124*, 4170–4171.
- (21) Park, G. Y.; Qayyum, M. F.; Woertink, J.; Hodgson, K. O.; Hedman, B.; Narducci Sarjeant, A. A.; Solomon, E. I.; Karlin, K. D. Geometric and Electronic Structure of [ $\{\text{Cu}(\text{MeAN})\}_2(\mu\text{-}\eta^2\text{-}\eta^2(\text{O}_2^{2-}))\}]^{2+}$  with an Unusually Long O–O Bond: O–O Bond Weakening vs Activation for Reductive Cleavage. *J. Am. Chem. Soc.* **2012**, *134*, 8513–8524.
- (22) Company, A.; Gómez, L.; Mas-Ballesté, R.; Korendovych, I. V.; Ribas, X.; Poater, A.; Parella, T.; Fontrodona, X.; Benet-Buchholz, J.; Solà, M.; Que, L.; Rybak-Akimova, E. V.; Costas, M. Fast O<sub>2</sub> Binding at Dicopper Complexes Containing Schiff-Base Dinucleating Ligands. *Inorg. Chem.* **2007**, *46*, 4997–5012.
- (23) Utz, D.; Heinemann, F. W.; Hampel, F.; Richens, D. T.; Schindler, S. Syntheses and Characterization of Two Dioxygen-Reactive Dinuclear Macrocyclic Schiff-Base Copper(I) Complexes. *Inorg. Chem.* **2003**, *42*, 1430–1436.
- (24) Matoba, Y.; Kumagai, T.; Yamamoto, A.; Yoshitsu, H.; Sugiyama, M. Crystallographic evidence that the dinuclear copper center of tyrosinase is flexible during catalysis. *J. Biol. Chem.* **2006**, *281*, 8981–8990.
- (25) Garcia-Bosch, I.; Company, A.; Frisch, J. R.; Torrent-Sucarrat, M.; Cardellach, M.; Gamba, I.; Güell, M.; Casella, L.; Que, L.; Ribas, X.; Luis, J. M.; Costas, M. O<sub>2</sub> Activation and Selective Phenolate *ortho*-Hydroxylation by an Unsymmetric Dicopper  $\mu\text{-}\eta^1\text{-}\eta^1$ -Peroxido Complex. *Angew. Chem., Int. Ed.* **2010**, *49*, 2406–2409.
- (26) Santagostini, L.; Gullotti, M.; Monzani, E.; Casella, L.; Dillinger, R.; Tuzek, F. Reversible dioxygen binding and phenol oxygenation in a tyrosinase model system. *Chem. - Eur. J.* **2000**, *6*, 519–522.
- (27) Palavicini, S.; Granata, A.; Monzani, E.; Casella, L. Hydroxylation of phenolic compounds by a peroxodicopper(II) complex: Further insight into the mechanism of tyrosinase. *J. Am. Chem. Soc.* **2005**, *127*, 18031–18036.
- (28) Schatz, M.; Leibold, M.; Foxon, S. P.; Weitzer, M.; Heinemann, F. W.; Hampel, F.; Walter, O.; Schindler, S. Syntheses and characterization of copper complexes of the ligand (2-aminoethyl)bis(2-pyridylmethyl)-amine (uns-penp) and derivatives. *Dalton Trans.* **2003**, 1480–1487.
- (29) For a precedent of a related unsymmetric Cu<sub>2</sub>O<sub>2</sub> system, see: Tachi, Y.; Aita, K.; Teramae, S.; Tani, F.; Naruta, Y.; Fukuzumi, S.; Itoh, S. Dicopper–Dioxygen Complex Supported by Asymmetric Pentapyridine Dinucleating Ligand. *Inorg. Chem.* **2004**, *43*, 4558–4560.
- (30) Serrano-Plana, J.; Costas, M.; Company, A. Building Complexity in O<sub>2</sub>-Binding Copper Complexes. Site-Selective Metalation and Intermolecular O<sub>2</sub>-Binding at Dicopper and Heterometallic Complexes Derived from an Unsymmetric Ligand. *Inorg. Chem.* **2014**, *53*, 12929–12938.
- (31) Halfen, J. A.; Mahapatra, S.; Wilkinson, E. C.; Kaderli, S.; Young, V. G.; Que, L.; Zuberbuehler, A. D.; Tolman, W. B. Reversible Cleavage and Formation of the Dioxygen O–O Bond Within a Dicopper Complex. *Science* **1996**, *271*, 1397–1400.
- (32) Mahapatra, S.; Halfen, J. A.; Wilkinson, E. C.; Pan, G.; Cramer, C. J.; Que, L.; Tolman, W. B. A new intermediate in copper dioxygen chemistry: breaking the O–O bond to form a  $\{\text{Cu}_2(\mu\text{-O})_2\}^{2+}$  core. *J. Am. Chem. Soc.* **1995**, *117*, 8865–8866.
- (33) Yamaguchi, Y.; Hearing, V. J. Physiological factors that regulate skin pigmentation. *BioFactors* **2009**, *35*, 193–199.
- (34) Huang, C.; Ghavtadze, N.; Chattopadhyay, B.; Gevorgyan, V. Synthesis of Catechols from Phenols via Pd-Catalyzed Silanol-Directed C–H Oxygenation. *J. Am. Chem. Soc.* **2011**, *133*, 17630–17633.
- (35) Tolman, W. B. Making and breaking the dioxygen O–O bond: new insights from studies of synthetic copper complexes. *Acc. Chem. Res.* **1997**, *30*, 227–237.
- (36) Mirica, L. M.; Vance, M.; Rudd, D. J.; Hedman, B.; Hodgson, K. O.; Solomon, E. I.; Stack, T. D. P. Tyrosinase reactivity in a model

complex: An alternative hydroxylation mechanism. *Science* **2005**, *308*, 1890–1892.

(37) Company, A.; Palavicini, S.; Garcia-Bosch, I.; Mas-Balleste, R.; Que, L.; Rybak-Akimova, E. V.; Casella, L.; Ribas, X.; Costas, M. Tyrosinase-like reactivity in a  $\text{Cu}^{\text{III}}(\mu\text{-O})_2$  species. *Chem. - Eur. J.* **2008**, *14*, 3535–3538.

(38) Yamazaki, S.; Itoh, S. Kinetic evaluation of phenolase activity of tyrosinase using simplified catalytic reaction system. *J. Am. Chem. Soc.* **2003**, *125*, 13034–13035.

(39) Citek, C.; Lyons, C. T.; Wasinger, E. C.; Stack, T. D. P. Self-assembly of the oxy-tyrosinase core and the fundamental components of phenolic hydroxylation. *Nat. Chem.* **2012**, *4*, 317–322.

(40) Herres-Pawlis, S.; Verma, P.; Haase, R.; Kang, P.; Lyons, C. T.; Wasinger, E. C.; Florke, U.; Henkel, G.; Stack, T. D. P. Phenolate Hydroxylation in a Bis( $\mu$ -oxo)dicopper(III) Complex: Lessons from the Guanidine/Amine Series. *J. Am. Chem. Soc.* **2009**, *131*, 1154–1169.

(41) Itoh, S.; Kumei, H.; Taki, M.; Nagatomo, S.; Kitagawa, T.; Fukuzumi, S. Oxygenation of phenols to catechols by a ( $\mu$ -h<sup>2</sup>:h<sup>2</sup>-peroxo)dicopper(II) complex: Mechanistic insight into the phenolase activity of tyrosinase. *J. Am. Chem. Soc.* **2001**, *123*, 6708–6709.

(42) Garcia-Bosch, I.; Ribas, X.; Costas, M. Electrophilic Arene Hydroxylation and Phenol O-H Oxidations Performed by an Unsymmetric  $\mu$ - $\eta^1$ : $\eta^1$ -O<sub>2</sub>-Peroxo Dicopper(II) Complex. *Chem. - Eur. J.* **2012**, *18*, 2113–2122.

(43) Kieber-Emmons, M. T.; Ginsbach, J. W.; Wick, P. K.; Lucas, H. R.; Helton, M. E.; Lucchese, B.; Suzuki, M.; Zuberbuhler, A. D.; Karlin, K. D.; Solomon, E. I. Observation of a  $\text{Cu}^{\text{II}}(\mu$ -1,2-peroxo)/ $\text{Cu}^{\text{III}}(\mu$ -oxo)<sub>2</sub> Equilibrium and its Implications for Copper-Dioxygen Reactivity. *Angew. Chem., Int. Ed.* **2014**, *53*, 4935–4939.

(44) Réglie, M.; Jorand, C.; Waegell, B. Binuclear copper complex model of tyrosinase. *J. Chem. Soc., Chem. Commun.* **1990**, 1752–1755.

(45) Rolff, M.; Schottenheim, J.; Peters, G.; Tucek, F. The First Catalytic Tyrosinase Model System Based on a Mononuclear Copper(I) Complex: Kinetics and Mechanism. *Angew. Chem., Int. Ed.* **2010**, *49*, 6438–6442.

(46) Hoffmann, A.; Citek, C.; Binder, S.; Goos, A.; Rübhausen, M.; Troepfner, O.; Ivanović-Burmazović, I.; Wasinger, E. C.; Stack, T. D. P.; Herres-Pawlis, S. Catalytic phenol hydroxylation with dioxygen: extension of the tyrosinase mechanism beyond the protein matrix. *Angew. Chem., Int. Ed.* **2013**, *52*, 5398–5401.

(47) Esguerra, K. V. N.; Fall, Y.; Petitjean, L.; Lumb, J.-P. Controlling the Catalytic Aerobic Oxidation of Phenols. *J. Am. Chem. Soc.* **2014**, *136*, 7662–7668.

(48) Esguerra, K. V. N.; Fall, Y.; Lumb, J.-P. A Biomimetic Catalytic Aerobic Functionalization of Phenols. *Angew. Chem., Int. Ed.* **2014**, *53*, 5877–5881.

(49) Lemal, D. M. Perspective on Fluorocarbon Chemistry. *J. Org. Chem.* **2004**, *69*, 1–11.

(50) Battaini, G.; Monzani, E.; Casella, L.; Lonardi, E.; Tepper, A. W. J. W.; Canters, G. W.; Bubacco, L. Tyrosine-catalyzed oxidation of fluorophenols. *J. Biol. Chem.* **2002**, *277*, 44606–44612.

(51) Serrano-Plana, J.; Garcia-Bosch, I.; Miyake, R.; Costas, M.; Company, A. Selective Ortho-Hydroxylation–Defluorination of 2-Fluorophenolates with a Bis( $\mu$ -oxo)dicopper(III) Species. *Angew. Chem., Int. Ed.* **2014**, *53*, 9608–9612.

(52) Balasubramanian, R.; Smith, S. M.; Rawat, S.; Yatsunyk, L. A.; Stemmler, T. L.; Rosenzweig, A. C. Oxidation of methane by a biological dicopper centre. *Nature* **2010**, *465*, 115–119.